Tissue-engineered bone used in a rabbit model of lumbar intertransverse process fusion: A comparison of osteogenic capacity between two different stem cells

HAI WANG[1-4], YUE ZHOU[2], CHANG-QING LI[2], TONG-WEI CHU[2], JIAN WANG[2] and BO HUANG[2]

[1]Department of Orthopaedics, Xingsha Branch, Hunan Provincial People's Hospital, Changsha, Hunan 410000;
[2]Department of Orthopaedics, Xinqiao Hospital, The Third Military Medical University, Chongqing 400037;
[3]Department of Orthopaedic and Trauma Surgery, Hunan Provincial People's Hospital, Changsha, Hunan 410000;
[4]Faculty of Life Science, Kunming University of Science and Technology, Kunming, Yunnan 650093, P.R. China

Received November 4, 2017; Accepted March 15, 2019

DOI: 10.3892/etm.2020.8523

Abstract. Spinal fusion serves an important role in the reconstruction of spinal stability via restoration of the normal spinal sequence and relief of pain. Studies have demonstrated that the fusion rate is mainly associated with the osteogenic capacity of the implanted graft. Mesenchymal stem cells (MSCs) have been successfully isolated from human degenerated cartilage endplate (CEP) and designated as CEP-derived stem cells (CESCs). Previous studies have suggested that CESCs possesses *in vitro* and *in vivo* chondrogenic potential superior to that of bone marrow (BM)-MSCs. In addition, CESCs have shown a stronger *in vitro* osteogenic ability. The present study aimed to further determine the *in vivo* three-dimensional osteogenesis efficacy of CESCs for spinal fusion. Tissue-engineered bone grafts were transplanted into a rabbit model of posterolateral lumbar intertransverse process fusion using CESCs and BM-MSCs as seed cells composited with porous hydroxyapatite (PHA). The results of manual palpation and computed tomography (CT) scan reconstruction indicated that the CESCs/PHA group had a higher fusion rate than the BM-MSCs/PHA group, although the difference was not observed to be statistically significant. In addition, RT-qPCR results revealed that the *in vitro* CESCs/PHA composite expressed significantly higher levels of osteogenic-specific mRNA compared with the BM-MSCs/PHA composite. Finally, micro-CT and semi-quantitative histological analysis further demonstrated that the newly formed bone quality of the CESCs/PHA group was significantly higher than that of the BM-MSCs/PHA group in the intertransverse process fusion model. Therefore, the study indicated that CESCs possess superior *in vivo* osteogenesis capacity compared with BM-MSCs, and might serve as an important alternative seed cell source for bone tissue engineering. These results may provide the foundation for a biological solution to spinal fusion or other bone defect issues.

Correspondence to: Dr Bo Huang or Dr Yue Zhou, Department of Orthopaedics, Xinqiao Hospital, The Third Military Medical University, 183 Xinqiao Street, Chongqing 400037, P.R. China
E-mail: fmmuhb@126.com

Key words: cartilage endplate-derived stem cells, porous hydroxyapatite, bone tissue engineering, lumbar intertransverse process fusion, osteogenic capacity, comparison

Introduction

From the pathological standpoint, in several diseases, including spondylosis, deformity, tumor, infection, fracture and instability, it is necessary to reconstruct a stable structure and correct an abnormal relationship between adjacent vertebral structures (1). Spinal fusion may enhance the mechanical stability of the spine via reconstruction and stabilization of the vertebral column; therefore, spinal fusion is currently one of the main treatment options for the aforementioned diseases (2,3). Until now, autografts have been the gold standard for use as spinal fusion materials; however, limited bone graft sources and donor-site morbidity hinder their extensive use, especially for those cases in which large amounts of bone graft material are required. By contrast, allograft and xenogenic bone, and other potential options for bone graft substitution or supplementation, including ceramics, calcium phosphate compounds, collagen gel and demineralized bone matrix, have shown significant variability in osteoinductive properties and clinical efficacy (4-6). Certain biological factors, such as bone morphogenetic protein have shown similar or improved fusion rates compared with autografts; however, potential safety concerns require further clarification (5). With the development of tissue engineering as an alternative approach for spinal fusion, bone tissue engineering has become a topic of particular interest (7,8).

The elements of tissue engineering comprise seed cells, biological scaffolding and growth factors. Seed cells serve an important role in the effects of tissue engineering technology (9). As classical seed cells, bone marrow mesenchymal stem cells (BM-MSCs) have frequently been employed in bone tissue engineering due to their multi-lineage differentiation

potential and rapid *in vitro* amplification (10,11). MSCs have been reported to exist in many types of mesenchymal tissue, and different tissue-derived MSCs differ from each other in properties including proliferation and differentiation potential, and tissue regeneration capacity (12,13). Therefore, specific types of MSCs should be chosen as appropriate for the intended tissue engineering application.

The intervertebral disc (IVD) is composed of annulus fibrosus (AF), nucleus pulposus (NP) and cartilage endplate (CEP). Previous studies reported that different types of MSCs exist in AF and NP regions (14,15). The present research team identified MSCs in CEP, which they designated as CEP-derived stem cells (CESCs), and found that CESCs share similar morphology, proliferation rate, cell cycle, immunophenotype and stem cell gene expression with BM-MSCs (16). Furthermore, CESCs have exhibited superior chondrogenic and osteogenic potentials compared with BM-MSCs *in vitro* (16,17). In an *in vivo* study, CESCs showed more powerful NP regeneration potential compared with AF-derived stem cells, NP-derived stem cells and BM-MSCs derived from the same patient following transplantation into the rabbit IVD, and displayed no obvious immune rejection as heterografts (18). However, the osteogenic characteristics of CESCs *in vivo* are unclear. Large quantities of CEP samples that are usually discarded as clinical waste in spinal fusion surgeries could be collected and reused for the extraction of CESCs, and may serve as an adequate seed cell source for experimental or clinical studies. Therefore, it is necessary to investigate the *in vivo* bone formation capacity of CESCs, and explore whether they have the potential to serve as seed cells for bone tissue engineering.

In the present study, CESCs and BM-MSCs were harvested from the same donors who received a lumbar spinal fusion procedure. After culturing and expanding, the cells were each seeded into porous hydroxyapatite (PHA). After 14 days *in vitro* induction, the cell/PHA composites were tested to determine the difference in osteogenic mRNA expression between the two types of seed cells. In addition, cell/PHA composites were implanted into a rabbit lumbar intertransverse process fusion model after 3 days *in vitro* induction. Eight weeks later, those grafts were gross observed, palpated and inspected with three-dimensional (3D) computed tomography (CT) reconstruction, micro-CT and quantitative histology to obtain bone formation indices for the comparison of *in vivo* osteogenic capacity.

Materials and methods

Ethics statement. All procedures were approved by the Institutional Review Board of Xinqiao Hospital and the patients provided written informed consent in the study before surgery. All animal experiments were also approved by the Xinqiao Hospital Committee on Ethics for the Care and Use of Laboratory Animals.

Isolation and culture of CESCs. The procedures for the isolation and culture of CESCs were performed as previously described (17,18). CEP samples were derived from 11 patients (age range: 37.9-61.2 years) who received lumbar fusion surgery at Xinqiao Hospital (Chongqing, China) between June 2015 and August 2016. The severity of CEP damage was determined as described by Rajasekaran *et al* (19). The characteristics of the patients and the tests in which their CESCs were used are shown in Table I.

Isolation and culture of BM-MSCs. Bone marrow samples were obtained from the aforementioned patients. Isolation and culture procedures for BM-MSCs were performed as previously described (20,21). In brief, 6 ml bone marrow was aspirated from the iliac crest and centrifuged at 900 x g for 25 min at 20˚C with an equal volume of 1.073 g/ml Percoll solution (Sigma-Aldrich; Merck KGaA). Mononuclear cells were carefully extracted and rinsed twice with PBS. Finally, the cells were suspended with DMEM/F12 (Hyclone) supplemented with 10% fetal calf serum (FCS; Hyclone) and 100 U/ml penicillin-streptomycin (Hyclone), then cultured in 25-cm^2 cell culture flasks (Costar; Corning, Inc.) with an atmosphere of 5% CO_2 at 37˚C. Thereafter, the culture medium was refreshed every 3 days. When 90% confluence was reached, the cells were passaged.

Determination of the cell surface antigen profile. BM-MSCs and CESCs from 3 patients were analyzed to determine their respective surface immunophenotypes by flow cytometry. Cells were washed with PBS twice and fixed with 4% paraformaldehyde at 4˚C for 10 min, then were incubated in the dark for 20 min with fluorescein isothiocyanate (FITC)-coupled monoclonal antibodies: CD11b-FITC, CD34-FITC, CD45-FITC, CD90-FITC, and CD105-FITC. The cells were then washed with PBS twice and re-suspended in 200 μl PBS. Finally, the cell suspension was passed through a Flow Cytometer, and the antigen phenotype was analyzed using Flow Jo software (version 7.5, Flow Jo LLC). Mouse isotype antibodies were used as controls.

Stem cell seeding in the PHA graft. BM-MSCs and CESCs derived from 8 patients were trypsinized, rinsed and re-suspended in fresh medium. After microscopic counting, $3x10^6$ cells were dropped into PHA (1.0x1.0x3.0 cm; porosity 42.2±1.8%; average pore diameter 180±60 μm) and centrifuged at 80 x g for 1 min at 20˚C. Cells/PHA grafts were incubated in an incubator with 5% CO_2 at 37˚C for 24 h. Then, they were induced for 2 weeks with basal medium supplemented with 100 nM dexamethasone, 0.2 mM ascorbate and 10 mM β-glycerophosphate (Sigma-Aldrich; Merck KGaA). During the induction period, the osteogenic medium was changed every 3 days.

Quantitative assay of alkaline phosphatase (ALP) activity. To quantify the ALP activity of the *in vitro* cultured grafts, a modified procedure was used (22). After induction for 1 or 2 weeks in the osteogenic medium, the grafts were washed with PBS, and then incubated in 1.0 ml lysis solution comprising 10 mM Tris-HCl, 1 mM $MgCl_2$ and 1% Triton X-100 at 4˚C. The supernatant was transferred to a 96-well plate (50 μl/well), and incubated with 100 μl substrate (*p*-nitrophenyl phosphate; 6.7 mM/l) at room temperature for 10 min. Then, 100 μl NaOH (0.1 M) was added to stop the reaction. The optical density (OD) at 405 nm (OD_{405}) was measured using a spectrophotometer. The OD_{405} value of a PHA graft containing no cells served as control, and each sample was tested in triplicate.

Table I. Characteristics of the patients enrolled in the study.

Case no.	Age (years)	Sex	Symptoms	Diagnosis	Disc level	CEPDT	Test item
1	54	F	BP-RP	Spondylolisthesis	L5/S1	VI	FC
2	57	M	BP-RP	Lumbar disc herniation	L5/S1	V	3D culture
3	56	F	BP-RP	Lumbar disc herniation	L4/5	V	3D culture
4	61	M	BP	Spondylolisthesis	L5/S1	V	FC
5	62	F	BP	Spondylolisthesis	L4/5	VI	*In vivo*
6	56	F	BP	Lumbar discogenic pain	L4/5	V	*In vivo*
7	51	F	BP	Spondylolisthesis	L5/S1	V	*In vivo*
8	58	M	BP-RP	Spondylolisthesis	L5/S1	VI	FC
9	56	F	BP-RP	Spondylolisthesis	L4/5	V	3D culture
10	54	F	BP-RP	Spondylolisthesis	L5/S1	VI	*In vivo*
11	51	F	BP-RP	Spondylolisthesis	L5/S1	V	*In vivo*

BP, back pain; RP, radicular pain; CEPDT, cartilage endplate damage type; FC, flow cytometry.

Table II. Primer sequences and procedure parameters used in the qPCR analysis.

Gene name	Primer sequences (5' to 3')	Ta (˚C)	Cycles (n)
β-actin	GTGGGGCGCCCCAGGCACCA (forward) CTTCCTTAATGTCACGCACGATTTC (reverse)	56	42
OC	ATGAGAGCCCTCACACTCCTC (forward) GCCGTAGAAGCGCCGATAGGC (reverse)	60	28
Runx2	ACGACAACCGCACCATGGT (forward) CTGTAATCTGACTCTGTCCT (reverse)	60	28
ALP	TGGAGCTTCAGAAGCTCAACACCA (forward) ATCTCGTTGTCTGAGTACCAGTCC (reverse)	58	30
OPN	AGAATGCTGTGTCCTCTGAAG (forward) GTTCGAGTCAATGGAGTCCTG (reverse)	59	29
BSP	AAGGCTACGATGGCTATGATGGT (forward) AATGGTAGCCGGATGCAAAG (reverse)	61	30

Ta, annealing temperature; OC, osteocalcin; ALP, alkaline phosphatase; OPN, osteopontin; BSP, bone sialoprotein.

Reverse transcription-quantitative reverse transcriptase polymerase chain reaction (RT-qPCR) assay. To evaluate the expression of osteogenic-specific genes in cells/PHA grafts *in vitro*, RT-qPCR was used (23). Stem cells harvested from 3 patients were each assigned to a PHA graft. After 2 weeks of induction, total RNA was extracted from each cell/PHA graft using a Total RNA Extraction kit (Qiagen GmbH) (24). RNA concentration and quality were evaluated on the basis of the OD 260/280 ratio. The mRNA (1.0 μl) was reversely transcribed to cDNA using a First Strand cDNA kit (Qiagen GmbH) according to the manufacturer's instructions. A total reaction volume of 25 μl containing SYBR-Green Master Mix reagent (Applied Biosystems; Thermo Fisher Scientific, Inc.) was amplified via qPCR (ABI Prism 7000; Thermo Fisher Scientific, Inc.). The following thermocycling conditions were used for the qPCR: Initial denaturation at 95˚C for 30 sec; 40 cycles of 95˚C for 5 sec and 60˚C for 32 sec; and a final dissociation stage at 95˚C for 15 sec, 60˚C for 60 sec and 95˚C for 15 sec. The osteogenic-specific genes and reaction conditions are shown in Table II, and β-actin served as an internal control to normalize the expression of the mRNA of these genes in different cell types. The quantitative determination of target mRNA expression was conducted according to the $2^{-\Delta\Delta Cq}$ method as previously described (24,25).

Animal model. An animal model was produced using previously reported methods (26,27). A total of 24 New Zealand white rabbits (The Third Military Medical University; age range 8-12 weeks), of mixed sexes (13 mala and 11 female) weighing 2.0-2.5 kg were used in the study. Rabbits were fed with rabbit pellets and drinking water *ad libitum* and reared in a constant temperature room at 20˚C with 50±5% humidity, 0.03% CO_2 and 12-h light/dark cycles. The rabbits were randomly divided into 3 groups (each n=8) as follows: BM-MSCs/PHA grafts; CESCs/PHA grafts; and PHA only grafts containing no cells to serve as a control. The rabbits

were anesthetized with sodium pentobarbital (30 mg/kg) via intravenous injection. Following removal of all the soft tissues, decortication of transverse process L4-L5 was performed to provide the fusion bed. Then, grafts that had undergone 3 days *in vitro* induction were implanted into bilateral sides of the intertransverse process interval, in parallel with the spine. Finally, the surgical incision was closed layer by layer.

Spiral CT scanning. To evaluate bone formation and fusion conditions, spiral CT scanning was conducted at 8 weeks after implantation surgery. The lumbar spine segment L3-L6 was scanned at 1-mm slice thickness and reconstructed into 3D images (SOMATOM Emotion; Siemens Healthineers). To observe the fusion conditions, 5 axial slices were scanned at positions containing the L4 and L5 transverse process attachments to the graft, and three intermediate regions, respectively.

Manual palpation. At 8 weeks after implantation, animals were sacrificed with an overdose of sodium pentobarbital. The objective lumbar spine (L4-L5 processes) was exposed after the removal of soft tissues, then manually palpated as previously described (28,29). Only if no movement was detected in the L4-L5 segment, and was confirmed by two checkers in a blinded manner, was the implanted graft considered as fused.

Micro-CT analysis. To assess the quality of the newly formed bone in the grafts, micro-CT was used (29,30). At 8 weeks after implantation, all the extraneous vertebrae and soft tissues were dissected, and the implants were scanned using micro-CT (GE Healthcare, Canada) using the following parameters: 60 kV; 0.6 mm aluminum filter; 800 μA; number of players=150. More than 1,000 axial images were obtained from each graft at the threshold of 1,200 HU. The region of interest was chosen symmetrically in the left and right grafts as a cylinder (0.5x0.5x0.5 cm^3) at rdifferent coronary positions. The grafts were equally portioned into five segments by 4 cross-sections. To evaluate osteogenesis, six morphometric indices were measured as follows: i) bone mineral density (BMD); ii) bone mineral content (BMC); iii) tissue mineral density (TMD); iv) tissue mineral content (TMC); v) bone volume fraction (BVF); vi) bone volume (BV) (30,31). PHA containing no stem cells served as control. Two photographers analyzed the data in a blinded manner.

Histological analysis. Animals were sacrificed with an overdose of sodium pentobarbital at 8 weeks after implantation. The graft specimen was harvested, fixed in 10% neutral buffered formalin for 24 h at 20˚C and sequentially dehydrated in ethanol solutions. Then, the graft was embedded in polymethylmethacrylate solution for 1 week. Grafts were sectioned to 50 μm using a diamond saw (Leica Microsystems GmbH, Germany). The slices were stained with Villanueva-Goldner's trichrome (VG) at 20˚C for 30 min and observed with a light microscope (Olympus Corporation) to evaluate osteogenesis by two pathologists in a blinded manner. A total of 9 sections from 3 grafts, with 3 random sections obtained from each graft, were quantitatively analyzed for newly formed bone and collagen I in VG staining using Image-Pro Plus software 6.0 (Media Cybernetics, Inc.). Osteogenesis was quantified on the basis of the area volume of light blue and red staining, which represented collagen I and newly formed trabecular bone, respectively (32).

Statistical analysis. SPSS version 13.0 software (IBM Corp.) was used for statistical analysis. All data are presented as the mean ± standard deviation. The two-tailed Student's t-test was used when comparing only two groups, and one-way ANOVA followed by Fisher's Least Significant Difference or Bonferroni's correction post-hoc tests were used to analyze differences among three groups. $P<0.05$ was considered to indicate a statistically significant difference.

Results

Cell morphology and antigenic phenotype. The BM-MSCs and CESCs exhibited a similar spindle-shaped appearance while in culture (passage 2; Fig. 1A). Flow cytometric analysis indicated that CESCs and BM-MSCs shared an analogous antigenic phenotype (Fig. 1B and C). Both cell types were negative for CD34, CD11b and CD45 (<2%), positive for CD90, and moderately positive for CD105. No marked differences were detected in the expression levels of CD11b, CD90, CD34 and CD45 between the two cell types.

ALP activity. The ALP activity results indicated that the OD_{405} values of both two cell types contained in the grafts increased from 1 to 2 weeks of induction (Fig. 2A). At the 1-week culture time point, the OD_{405} value of the CESCs/PHA group was significantly higher compared with that of the BM-MSCs/PHA group (1.80±0.26 vs. 1.47±0.24; $P<0.01$; Fig. 2A). A significant difference was also detected between the two groups at 2 weeks (2.36±0.28 vs. 1.92±0.25; $P<0.01$; Fig. 2A).

Osteogenic capacity in 3D culture. According to the RT-qPCR assay results, after 2 weeks of induction, the CESCs/PHA group exhibited a significantly higher expression level of ALP mRNA compared with the BM-MSCs/PHA group (1.45±0.20 vs. 1.0-fold; $P<0.01$; Fig. 2B). For Runx2 and osteocalcin (OC) mRNA, significantly higher expression was also observed in the CESCs/PHA group compared with the BM-MSCs/PHA group (1.19±0.18 vs. 1.0-fold for Runx2; 1.24±0.20 vs. 1.0 for OC; $P<0.01$; Fig. 2B). However, both groups exhibited comparable expression levels for osteopontin and bone sialoprotein mRNA ($P>0.05$; Fig. 2B).

3D CT evaluation and fusion status. Although all grafts broke into several parts during surgery, at 8 weeks after implantation, reconstructed 3D CT demonstrated bony healing of the fractured segments and definite fusion existing between the transverse processes (L4 and L5) and the graft in the majority of the cell-containing grafts (Fig. 3A and B).

Analysis using manual palpation revealed that 7/8 animals (87.50%) in the CESCs/PHA group and 6/8 animals (75.0%) in the BM-MSCs/PHA group achieved fusion; however, fusion was obtained in only 3/8 samples (37.5%) for the graft comprising only PHA. The fusion rate in the control group was lower compared with the CESCs/PHA and BM-MSCs/PHA groups ($P<0.05$). Furthermore, no significant difference in fusion rate was detected between the CESCs/PHA and BM-MSCs/PHA groups ($P>0.05$; Fig. 3C).

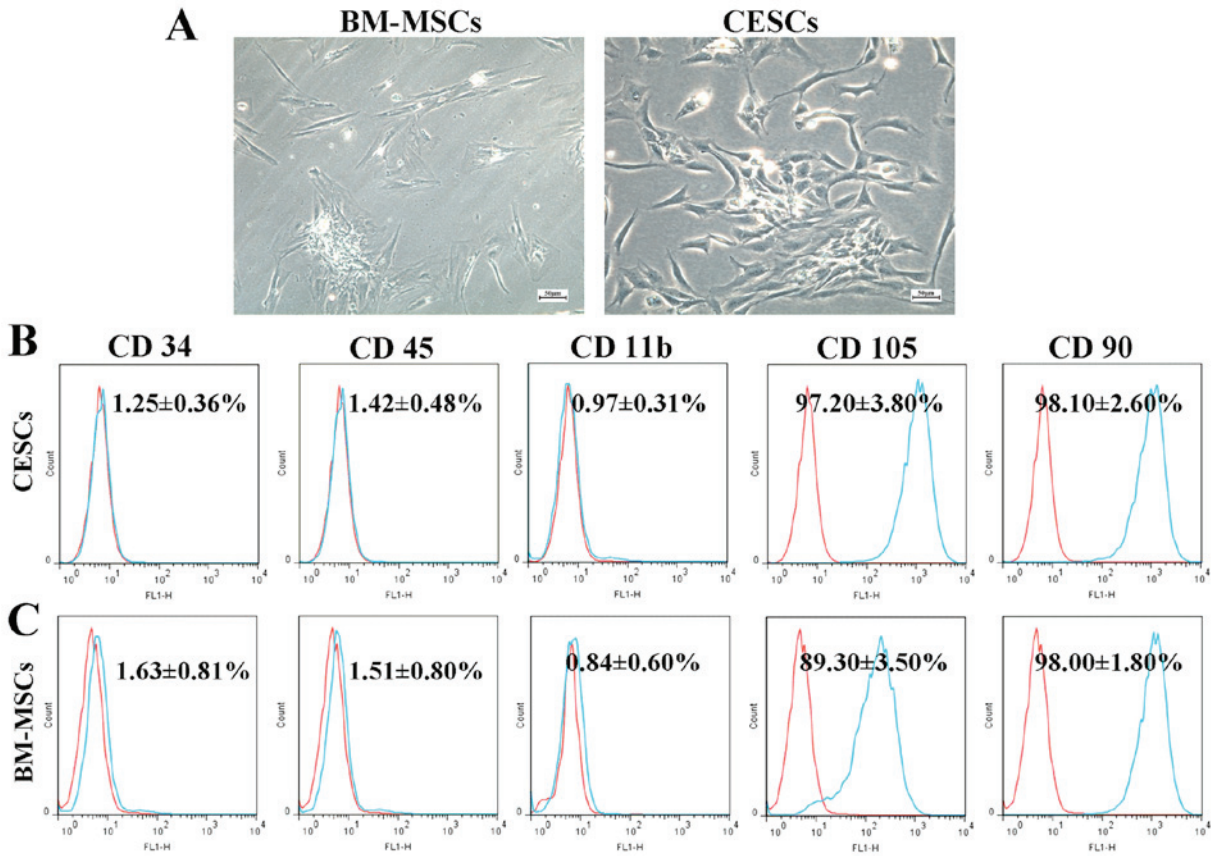

Figure 1. BM-MSCs and CESCs share similar biological characteristics. (A) Morphological appearance of BM-MSCs and CESCs observed under a light microscope (scale bar=50 μm). Typical immunophenotypes of (B) CESCs and (C) BM-MSCs as revealed using flow cytometry. BM-MSCs, bone marrow mesenchymal stem cells; CESCs, cartilage endplate-derived stem cells.

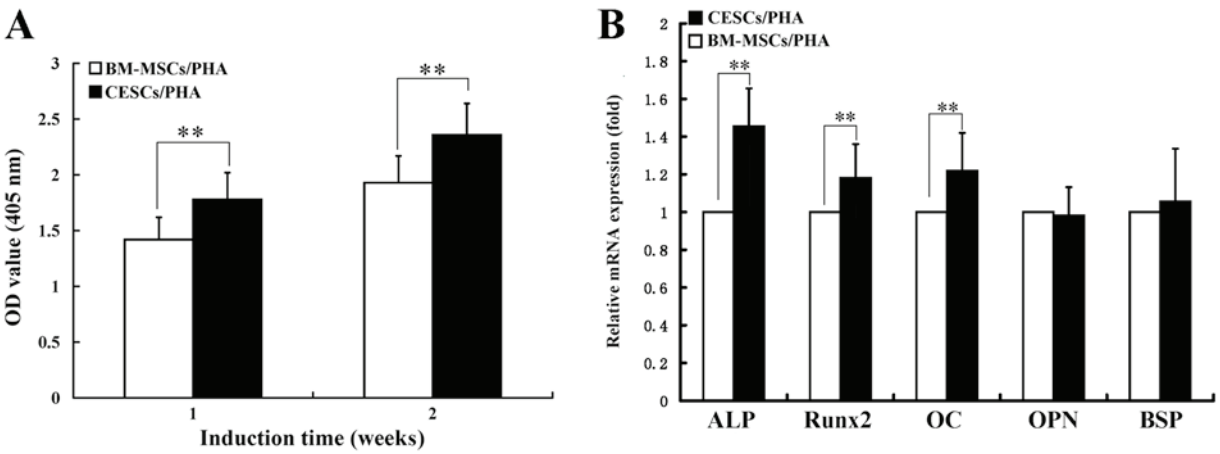

Figure 2. Osteogenic induction culture of PHA grafts seeded with cells. (A) In an alkaline phosphatase activity assay, CESCs/PHA grafts exhibited significantly higher OD_{405} values than BM-MSCs/PHA grafts after 1 and 2 weeks of induction. Data are from 3 grafts, each inoculated with cells from a different patient. (B) RT-qPCR evaluation of the expression levels of osteogenic mRNA by the grafts *in vitro* after 2 weeks of induction. The CESCs/PHA group exhibited significantly higher expression levels of ALP, Runx 2 and OC compared with the BM-MSCs/PHA group. No significant differences were detected in OPN and BSP expression levels between the two groups. **P<0.01. PHA, porous hydroxyapatite; CESCs, cartilage endplate-derived stem cells; BM-MSCs, bone marrow mesenchymal stem cells; OD, optical density.

Bone formation analysis by micro-CT. According to the micro-CT data, all the osteogenesis indices in the CESCs/PHA group had higher values compared with those of the BM-MSCs/PHA group (Fig. 4). Significant differences were observed between the two stem cell-containing groups for BV, BVF, BMC, BMD and TMD (P<0.01; Fig. 4B).

Histological assessment. In VG stained slices, collagen I, newly formed trabecular bone and PHA were stained as blue, red and black, respectively (Fig. 5A-F). The CESCs/PHA grafts exhibited more newly formed collagen I and trabecular bone than the BM-MSCs/PHA group. For the only PHA graft, the content of collagen I and trabecular bone was clearly

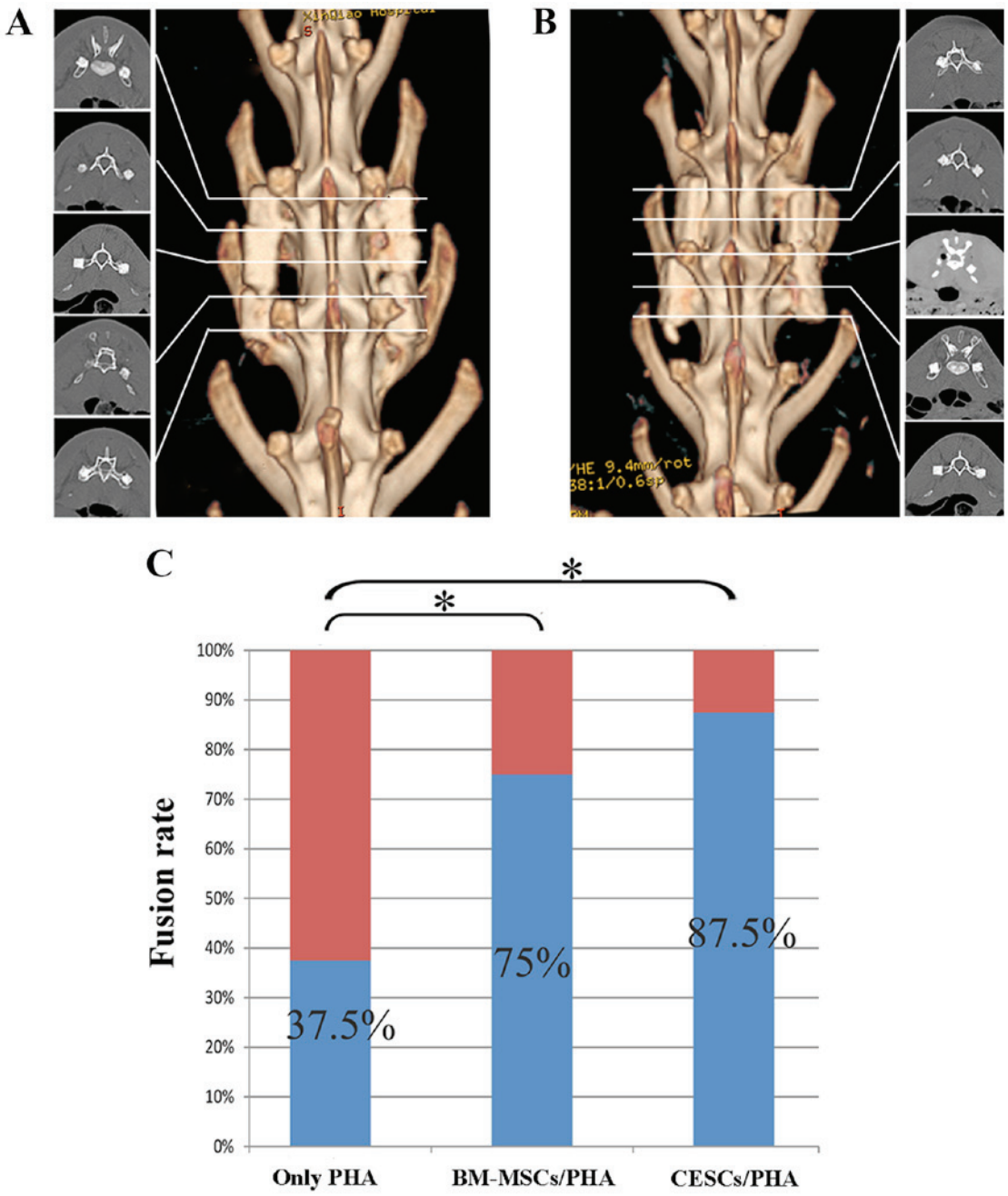

Figure 3. Spiral CT observation and three dimensional reconstruction of the grafts at 8 weeks after implantation, revealing bony healing of the fractured segments and fusion existing between the transverse processes (L4 and L5) and the grafts at 8 weeks after surgery. (A) BM-MSCs/PHA graft and its coronal scans. (B) CESCs/PH7A graft and its coronal scans. (C) Comparison of fusion rates in the only PHA, BM-MSCs/PHA and CESCs/PHA groups. *P<0.05 vs. control group. n=4. CT, computed tomography; PHA, porous hydroxyapatite; CESCs, cartilage endplate-derived stem cells; BM-MSCs, bone marrow mesenchymal stem cells.

the lowest. Quantitative data indicated that the CESCs/PHA group had 740±62 μm^2 newly formed trabecular bone and 863±84 μm^2 of collagen I, whereas the respective values in the BM-MSCs/PHA group were 381±36 and 740±54 μm^2, respectively (Fig. 5G). Significant differences were detected between each pair of the three groups for collagen I and trabecular bone (P<0.01).

Discussion

MSCs are an attractive cell population for use in the regeneration of various tissues due to their multilineage differentiation potential (10). Studies have indicated the extensive use of MSCs, especially BM-MSCs, in bone tissue engineering (8). The MSCs used in the present study were obtained using previously described methods (10,18). In addition, the cell surface antigen profiles were also basically consistent with those in previous studies, and indicate that the cells used in the present study possess the basic characteristics of MSCs described by the International Society for Cellular Therapy (18,33).

Generally, the degenerative status of NP and CEP is hemi-quantitatively judged by magnetic resonance imaging (34,35). In the present study, CESCs were obtained from human degenerated CEP of types V and VI according to the previously described classification (19). Whether the

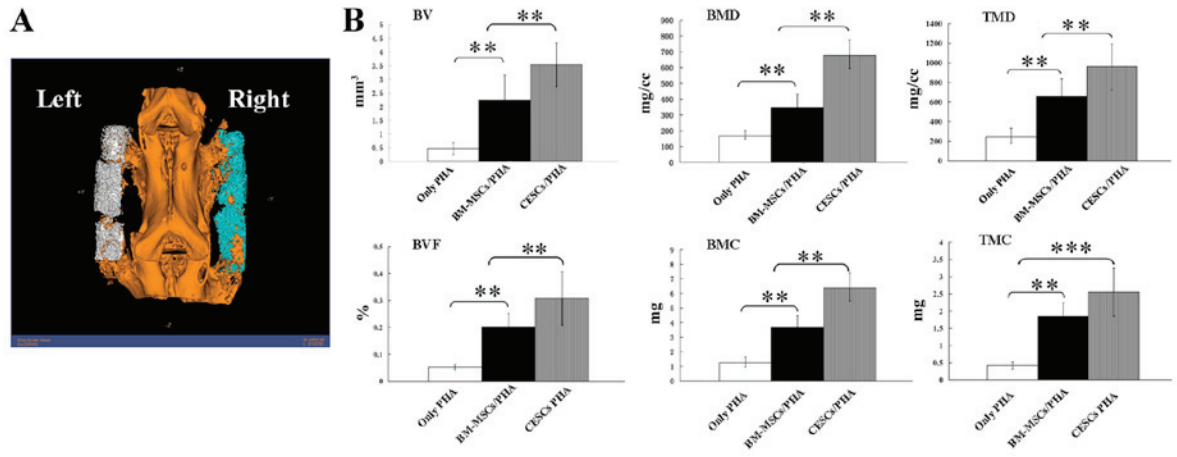

Figure 4. Assessment of newly formed bone quality using micro-CT. (A) Reconstructed three dimensional schematic diagram obtained by micro-CT. (B) Significant differences existed between the BM-MSCs/PHA and CESCs/PHA groups for BV, BVF, BMC, BMD and TMD (P<0.01). **P<0.01, ***P<0.001; n=8. PHA, porous hydroxyapatite; CESCs, cartilage endplate-derived stem cells; BM-MSCs, bone marrow mesenchymal stem cells; BV, bone volume; BVF, bone volume fraction; BMC, bone mineral content; BMD, bone mineral density; TMD, tissue mineral density; TMC, tissue mineral content.

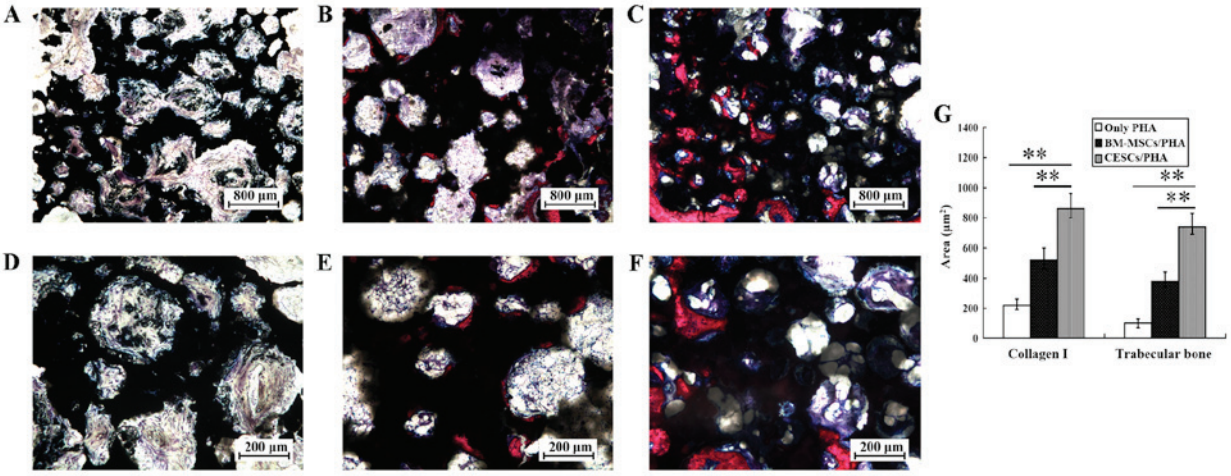

Figure 5. VG stained sections of grafts at 8 weeks after implantation. (A-F) Collagen I, trabecular bone and PHA are indicated by blue, red and black staining, respectively. Representative images of (A and D) only PHA, (B and E) BM-MSCs/PHA and (C and F) CESCs/PHA grafts are shown. The CESCs/PHA grafts exhibited higher volumes of collagen I and newly trabecular bone than the BM-MSCs/PHA grafts. The only PHA grafts served as control. (G) Quantitative data indicated that the CESCs/PHA group had 740±62 μm^2 newly formed trabecular bone and 863±84 μm^2 collagen I, whereas the respective areas for the BM-MSCs/PHA group were 381±36 and 740±54 μm^2, respectively. **P<0.01. n=8. VG, Villanueva-Goldner's trichrome; PHA, porous hydroxyapatite; CESCs, cartilage endplate-derived stem cells; BM-MSCs, bone marrow mesenchymal stem cells.

bone formation ability correlates with the degeneration level of the extracted sample remains to be elucidated. The possible discrepant biological characteristics and bone formation potential of the CESCs derived from clinical CEP samples with different degenerative degrees merits investigation in future studies.

Unlike 2D culturing, the 3D culture environment closely resembles the *in vivo* environment. Different growing conditions may lead to differences in biological characteristics. ALP mRNA expression and ALP activity were significantly upregulated in CESCs as compared with BM-MSCs in the present study, and were accordant in 2D and 3D culturing environments (16). OC as a marker for the late stage of osteoblast differentiation was expressed at a significantly highly level in CESCs/PHA compared with BM-MSCs/PHA, which was consistent with previous 2D culture data (16,36). In addition, significantly higher expression of Runx2, another specific matrix protein expression marker for bone maturation, was observed in CESCs/PHA compared with BM-MSCs/PHA in the 3D environment, whereas no significant difference was detected between CESCs and BM-MSCs in 2D culture (16,37). It is hypothesized that the aforementioned differences may be partially attributed to the favorable cell-cell and cell-extracellular matrix (ECM) interactions in a 3D multilayered-cell environment.

PHA is a classical scaffold material with good biocompatibility, bone induction and bone conduction properties, and is often used in bone tissue engineering research (38). The PHA used in the present study had a porosity of 42.2±1.8%, an average pore diameter of 180±60 μm, and a 3D framework in which cellular proliferation and differentiation, and ECM deposition may occur. However, the weak fracture resistance of PHA predisposes it to break under torsion or shear force (39). In the present study, nearly all PHA grafts broke into two to

four parts following transplantation into the intertransverse process. However, the broken grafts were restored to integrity by the newly formed bone that gradually bridged the defects of the broken material. Furthermore, the grafts with CESCs or BM-MSCs demonstrated significantly higher fusion rates compared with the PHA only control. Generally, in the present study, PHA breakage during the experimental process did not affect the evaluation of bone formation capacity. Instead, it further certified that the implanted stem cells, especially CESCs, provided a stronger osteogenic and repair capacity, even under the challenging environment caused by PHA breakage.

Micro-CT is a reliable *in vivo* method for the quantitative and qualitive evaluation of newly formed bone without physical disruption of the sample. Indices such as BV, BVF, BMC, BMD, TMC and TMD indirectly reflect fusion quality (40). In the CESCs/PHA group, BV, BVF, BMC, BMD and TMD values were significantly higher compared with those of the BM-MSCs/PHA group; only the TMC values exhibited no significant differences between these two groups. These results indicate that the CESCs/PHA complex was able to induce bone regeneration more efficiently. In addition, quantitative histology complemented the micro-CT data by revealing that the volume of collagen I, the main organic component of bone (41), and newly regenerated trabecular bone in the CESCs/PHA group were significantly higher than those in the BM-MSCs/PHA group. Therefore, the results of micro-CT and histological analysis confirmed that the CESCs/PHA composite enhanced the quantity and quality of bone formation.

However, the present study has certain limitations. Firstly, rabbits are relatively small in size, and the mechanical stress that the implanted grafts endured in rabbits are likely to differ from those in the human spine. Different mechanical factors might have a profound effect on the biological characteristics of seed cells, including their osteogenic capacities. Therefore, in subsequent studies, larger animals such as goats or nonhuman primates might be used to provide a more restrictive biomechanical environment that is more analogous to that of the human spine. Secondly, autologous bone grafting was not set as the gold standard in this study due to the small number of experimental animals; therefore, the final fusion efficacy that CESCs could achieve relative to the gold standard remains unknown. Thirdly, no biomechanical tests were performed to further assess the quality of the newly formed bones due to the small size of the rabbit spine. To address this issue, larger animals should be included in future studies.

To the best of our knowledge, the present study was the first to use stem cells derived from human degenerated CEP as seed cells for tissue-engineered bone products, and compare their osteogenesis with the traditional seed cells, BM-MSCs, in the 3D *in vitro* environment and *in vivo* rabbit spinal fusion model. Although the present study yielded encouraging results, the definite osteogenic efficacy relative to the gold standard and the long-term safety for *in vivo* implantation require further investigation prior to clinical application. In addition, PHA should be improved to enhance its fracture resistance, or an alternative scaffold with fine biocompatibility and mechanical properties should be considered for further study.

In conclusion, the present study preliminarily compared the osteogenic capacity between CESCs and BM-MSCs derived from the same donors in the rabbit lumbar intertransverse process fusion model. CESCs exhibited superior bone formation ability than BM-MSCs when used with PHA under a 3D environment *in vitro* and *in vivo*. The results indicate that CESCs have potential as an efficient and sufficient seed cell source for bone tissue engineering, and CESC-based products show promise as superior candidates for future clinical application in spinal fusion or other bone regeneration and repair issues.

Acknowledgements

Not applicable.

Funding

This study was supported by the National Natural Science Foundation of China (grant nos. 81472076 and 81560369).

Availability of data and materials

The datasets used and/or analyzed during the current study are available from the corresponding author on reasonable request.

Authors' contributions

HW performed the experiments, wrote the manuscript and collected, analyzed and interpreted data. YZ contributed to study design and conception, wrote the manuscript and analysed and interpreted data. CQL, TWC and JW performed the experiments and obtained clinical samples. BH contributed to study design and conception, analysed and interpreted data, and wrote and gave final approval of the manuscript. All authors read and approved the final manuscript.

Ethics approval and consent to participate

All procedures were approved by the Institutional Review Board of Xinqiao Hospital. All patients provided written informed consent for participation in the study. All animal experiments were approved by the Xinqiao Hospital Committee on Ethics for the Care and Use of Laboratory Animals.

Patient consent for publication

Not applicable.

Competing interests

All the authors declare that they have no competing interests.

References

1. Kawakami N, Tsuji T, Imagama S, Lenke LG, Puno RM, Kuklo TR and Spinal Deformity Study Group: Classification of congenital scoliosis and kyphosis: A new approach to the three-dimensional classification for progressive vertebral anomalies requiring operative treatment. Spine (Phila Pa 1976) 34: 1756-1765, 2009.
2. An H, Boden SD, Kang J, Sandhu HS, Abdu W and Weinstein J: Summary statement: Emerging techniques for treatment of degenerative lumbar disc disease. Spine (Phila Pa 1976) 28 (Suppl 15): S24-S25, 2003.

3. Hidaka C, Goshi K, Rawlins B, Boachie-Adjei O and Crystal RG: Enhancement of spine fusion using combined gene therapy and tissue engineering BMP-7-expressing bone marrow cells and allograft bone. Spine (Phila Pa 1976) 28: 2049-2057, 2003.
4. Boden SD: Overview of the biology of lumbar spine fusion and principles for selecting a bone graft substitute. Spine (Phila Pa 1976) 27 (Suppl 1): S26-S31, 2002.
5. Rihn JA, Kirkpatrick K and Albert TJ: Graft options in posterolateral and posterior interbody lumbar fusion. Spine (Phila Pa 1976) 35: 1629-1639, 2010.
6. Minamide A, Yoshida M, Kawakami M, Yamasaki S, Kojima H, Hashizume H and Boden SD: The use of cultured bone marrow cells in type I collagen gel and porous hydroxyapatite for posterolateral lumbar spine fusion. Spine (Phila Pa 1976) 30: 1134-1138, 2005.
7. Szpalski C, Barbaro M, Sagebin F and Warren SM: Bone tissue engineering: Current strategies and techniques-part II: Cell types. Tissue Eng Part B Rev 18: 258-269, 2012.
8. Seong JM, Kim BC, Park JH, Kwon IK, Mantalaris A and Hwang YS: Stem cells in bone tissue engineering. Biomed Mater 5: 062001, 2010.
9. Bruder SP and Fox BS: Tissue engineering of bone: Cell based strategies. Clin Orthop Relat Res: (Suppl 367) S68-S83, 1999.
10. Pittenger MF, Mackay AM, Beck SC, Jaiswal RK, Douglas R, Mosca JD and Moorman MA: Multilineage potential of adult human mesenchymal stem cells. Science 284: 143-147, 1999.
11. Jones E and McGonagle D: Human bone marrow mesenchymal stem cells in vivo. Rheumatology 47: 126-131, 2008.
12. Chamberlain G, Fox J, Ashton B and Middleton J: Concise review: Mesenchymal stem cells: Their phenotype, differentiation capacity, immunological features, and potential for homing. Stem Cells 25: 2739-2749, 2007.
13. Uccelli A, Moretta L and Pistoia V: Mesenchymal stem cells in health and disease. Nat Rev Immunol 8: 726-736, 2008.
14. Blanco JF, Graciani IF, Sanchez-Guijo FM, Muntion S, Hernandez-Campo P, Santamaria C, Carrancio S, Barbado MV, Cruz G, Gutierrez-Cosío S, *et al*: Isolation and characterization of mesenchymal stromal cells from human degenerated nucleus pulposus: Comparison with bone marrow mesenchymal stromal cells from the same subjects. Spine (Phila Pa 1976) 35: 2259-2265, 2010.
15. Feng G, Yang X, Shang H, Marks IW, Shen FH, Katz A, Arlet V, Laurencin CT and Li X: Multipotential differentiation of human anulus fibrosus cells: An in vitro study. J Bone Joint Surg Am 92: 675-685, 2010.
16. Liu LT, Huang B, Li CQ, Zhuang Y, Wang J and Zhou Y: Characteristics of stem cells derived from the degenerated human intervertebral disc cartilage endplate. PLoS One 6: e26285, 2011.
17. Huang B, Liu LT, Li CQ, Zhuang Y, Luo G, Hu SY and Zhou Y: Study to determine the presence of progenitor cells in the degenerated human cartilage endplates. Eur Spine J 21: 613-622, 2012.
18. Wang H, Zhou Y, Huang B, Liu LT, Liu MH, Wang J, Li CQ, Zhang ZF, Chu TW and Xiong CJ: Utilization of stem cells in alginate for nucleus pulposus tissue engineering. Tissue Eng Part A 20: 908-920, 2014.
19. Rajasekaran S, Venkatadass K, Naresh Babu J, Ganesh K and Shetty AP: Pharmacological enhancement of disc diffusion and differentiation of healthy, ageing and degenerated discs: Results from in-vivo serial post-contrast MRI studies in 365 human lumbar discs. Eur Spine J 17: 626-643, 2008.
20. Bilic G, Zeisberger SM, Mallik AS, Zimmermann R and Zisch AH: Comparative characterization of cultured human term amnion epithelial and mesenchymal stromal cells for application in cell therapy. Cell Transplant 17: 955-968, 2008.
21. Lubis AM, Sandhow L, Lubis VK, Noor A, Gumay F, Merlina M, Yang W, Kusnadi Y, Lorensia V, Sandra F and Susanto NH: Isolation and cultivation of mesenchymal stem cells from iliac crest bone marrow for further cartilage defect management. Acta Med Indones 43: 178-184, 2011.
22. Jackson WM, Aragon AB, Bulken-Hoover JD, Nesti LJ and Tuan RS: Putative heterotopic ossification progenitor cells derived from traumatized muscle. J Orthop Res 27: 1645-1651, 2009.
23. Ripamonti U, Klar RM, Renton LF and Ferretti C: Synergistic induction of bone formation by hOP-1, hTGF-beta3 and inhibition by zoledronate in macroporous coral-derived hydroxyapatites. Biomaterials 31: 6400-6410, 2010.
24. Jeon O, Rhie JW, Kwon IK, Kim JH, Kim BS and Lee SH: In vivo bone formation following transplantation of human adipose-derived stromal cells that are not differentiated osteogenically. Tissue Eng Part A 14: 1285-1294, 2008.
25. Livak KJ and Schmittgen TD: Analysis of relative gene expression data using real-time quantitative PCR and the 2(-Delta Delta C(T)) method. Methods 25: 402-408, 2001.
26. Alanay A, Chen C, Lee S, Murray SS, Brochmann EJ, Miyazaki M, Napoli A and Wang JC: The adjunctive effect of a binding peptide on bone morphogenetic protein enhanced bone healing in a rodent model of spinal fusion. Spine (Phila Pa 1976) 33: 1709-1713, 2008.
27. Boden SD, Schimandle JH and Hutton WC: An experimental lumbar intertransverse process spinal fusion model. Radiographic, histologic, and biomechanical healing characteristics. Spine (Phila Pa 1976) 20: 412-420, 1995.
28. Grauer JN, Bomback DA, Lugo R, Troiano NW, Patel TC and Friedlaender GE: Posterolateral lumbar fusions in athymic rats: Characterization of a model. Spine J 4: 281-286, 2004.
29. Miyazaki M, Zuk PA, Zou J, Yoon SH, Wei F, Morishita Y, Sintuu C and Wang JC: Comparison of human mesenchymal stem cells derived from adipose tissue and bone marrow for ex vivo gene therapy in rat spinal fusion model. Spine (Phila Pa 1976) 33: 863-869, 2008.
30. Sheyn D, Rüthemann M, Mizrahi O, Kallai I, Zilberman Y, Tawackoli W, Kanim LE, Zhao L, Bae H, Pelled G, *et al*: Genetically modified mesenchymal stem cells induce mechanically stable posterior spine fusion. Tissue Eng Part A 16: 3679-3686, 2010.
31. Hildebrand T, Laib A, Müller R, Dequeker J and Rüegsegger P: Direct three-dimensional morphometric analysis of human cancellous bone: Microstructural data from spine, femur, iliac crest, and calcaneus. J Bone Miner Res 14: 1167-1174, 1999.
32. Cinotti G, Patti AM, Vulcano A, Della Rocca C, Polveroni G, Giannicola G and Postacchini F: Experimental posterolateral spinal fusion with porous ceramics and mesenchymal stem cells. J Bone Joint Surg Br 86: 135-142, 2004.
33. Dominici M, Le Blanc K, Mueller I, Slaper-Cortenbach I, Marini F, Krause D, Deans R, Keating A, Prockop DJ and Horwitz E: Minimal criteria for defining multipotent mesenchymal stromal cells. The International Society for Cellular Therapy position statement. Cytotherapy 8: 315-317, 2006.
34. Pfirrmann CW, Metzdorf A, Zanetti M, Hodler J and Boos N: Magnetic resonance classification of lumbar intervertebral disc degeneration. Spine (Phila Pa 1976) 26: 1873-1878, 2001.
35. Kuisma M, Karppinen J, Haapea M, Lammentausta E, Niinimaki J and Tervonen O: Modic changes in vertebral endplates: A comparison of MR imaging and multislice CT. Skeletal Radiol 38: 141-147, 2009.
36. Yang F, Yuan PW, Hao YQ and Lu ZM: Emodin enhances osteogenesis and inhibits adipogenesis. BMC Complement Altern Med 14: 74, 2014.
37. Hassan MQ, Tare RS, Lee SH, Mandeville M, Morasso MI, Javed A, van Wijnen AJ, Stein JL, Stein GS and Lian JB: BMP2 commitment to the osteogenic lineage involves activation of Runx2 by DLX3 and a homeodomain transcriptional network. J Biol Chem 281: 40515-40526, 2006.
38. Oryan A, Alidadi S, Moshiri A and Maffulli N: Bone regenerative medicine: Classic options, novel strategies, and future directions. J Orthop Surg Res 9: 18, 2014.
39. Lee JH, Yu CH, Yang JJ, Baek HR, Lee KM, Koo TY, Chang BS and Lee CK: Comparative study of fusion rate induced by different dosages of Escherichia coli-derived recombinant human bone morphogenetic protein-2 using hydroxyapatite carrier. Spine J 12: 239-248, 2012.
40. Schulte FA, Lambers FM, Kuhn G and Muller R: In vivo micro-computed tomography allows direct three-dimensional quantification of both bone formation and bone resorption parameters using time-lapsed imaging. Bone 48: 433-442, 2011.
41. Miller A: Collagen: The organic matrix of bone. Philos Trans R Soc Lond B Biol Sci 304: 455-477, 1984.